Water Research 221 (2022) 118727

Contents lists available at ScienceDirect

Water Research

journal homepage: www.elsevier.com/locate/watres

Origin, accumulation and fate of dissolved organic matter in an extreme hypersaline shallow lake

A. Butturini [a,*], P. Herzsprung [b], O.J. Lechtenfeld [c], P. Alcorlo [d], R. Benaiges-Fernandez [e,j], M. Berlanga [f], J. Boadella [g], Z. Freixinos Campillo [h], R.M. Gomez [h], M.M. Sanchez-Montoya [h,i], J. Urmeneta [j,k], A.M. Romaní [g]

[a] Department de Biologia Evolutiva, Ecologia y Ciencies Ambientals, Universitat de Barcelona, Diagonal 643, Barcelona, Catalonia 08028, Spain
[b] Department of Lake Research, Helmholtz Centre for Environmental Research (UZF), Magdeburg, Germany
[c] Department of Analytical Chemistry, Research Group BioGeoOmics, Helmholtz Centre for Environmental Research (UZF), Leipzig, Germany
[d] Departamento de Ecología, Centro de Investigación en Biodiversidad y Cambio Global (CIBC), Universidad Autónoma de Madrid, Madrid, Spain
[e] Mineralogia Aplicada, Geoquímica i Geomicrobiologia (MAiMA), Departament de Mineralogia, Petrologia i Geologia Aplicada, Institut de Recerca de l'Aigua (IdRA), Universitat de Barcelona (UB), Barcelona, Spain
[f] Departament de Biologia, Sanitat i Medi Ambient, Universitat de Barcelona, Diagonal 643, Barcelona, Catalonia 08028, Spain
[g] Institute of Aquatic Ecology, University of Girona, Spain
[h] Department of Ecology and Hydrology, Faculty of Biology, University of Murcia, Campus de Espinardo, Murcia 30100, Spain
[i] Department of Biodiversity, Ecology, and Evolution, Faculty of Biological Sciences, Complutense University of Madrid, Calle Jose Antonio Novais, 12, Madrid 28040, Spain
[j] Department de Genética, Microbiología i Estadística, Universitat de Barcelona, Diagonal 643, Barcelona, Catalonia 08028, Spain
[k] Biodiversity Research Institute, University of Barcelona, Spain

ARTICLE INFO

Keywords:
Dissolved organic matter
Hypersaline waters
Endorheic
Spectroscopy
FT-ICR-MS

ABSTRACT

Hypersaline endorheic aquatic systems (H-SEAS) are lakes/shallow playas in arid and semiarid regions that undergo extreme oscillations in salinity and severe drought episodes. Although their geochemical uniqueness and microbiome have been deeply studied, very little is known about the availability and quality of dissolved organic matter (DOM) in the water column.. A H-SEAS from the Monegros Desert (Zaragoza, NE Spain) was studied during a hydrological wetting-drying-rewetting cycle. DOM analysis included: (i) a dissolved organic carbon (DOC) mass balance; (ii) spectroscopy (absorbance and fluorescence) and (iii) a molecular characterization with Fourier-transform ion cyclotron resonance mass spectrometry (FT-ICR-MS). The studied system stored a large amount of DOC and under the highest salinity conditions, salt-saturated waters (i.e., brines with salinity > 30%) accumulated a disproportionate quantity of DOC, indicating a significant *in-situ* net DOM production. Simultaneously, during the hydrological transition from wet to dry, the DOM pool showed strong alterations of it molecular composition. Spectroscopic methods indicated that aromatic and degraded DOM was rapidly replaced by fresher, relatively small, microbial-derived moieties with a large C/N ratio. FT-ICR-MS highlighted the accumulation of small, saturated and oxidized molecules (molecular O/C > 0.5), with a remarkable increase in the relative contribution of highly oxygenated (molecular O/C>0.9) compounds and a decrease of aliphatic and carboxyl-rich alicyclic moleculesThese results indicated that H-SEAS are extremely active in accumulating and processing DOM, with the notable release of organic solutes probably originated from decaying microplankton under large osmotic stress at extremely high salinities.

1. Introduction

Hypersaline endorheic aquatic systems (H-SEAS) are harsh and vulnerable ecosystems widely distributed in arid and semiarid regions worldwide (Wang et al., 2018) that undergo large oscillations in salinity, with maxima at the salt saturation level. Some recent geo-statistical estimates suggest that inland saline and hypersaline waters might account for 47% of global lakes volumes, and small saline waters bodies

* Corresponding author.
E-mail address: abutturini@ub.edu (A. Butturini).

https://doi.org/10.1016/j.watres.2022.118727
Received 21 March 2022; Received in revised form 19 May 2022; Accepted 6 June 2022
Available online 8 June 2022

might represent up to the 3% of global lakes volumes (Messager et al., 2016). H-SEAS attracted researches for hosting diverse and dynamic halophilic consortiums of archaea, bacteria, plankton, fungi, protists and invertebrates (Lee et al., 2018; Menéndez-Serra et al., 2021; Belilla et al., 2021). By contrast, information about dissolved organic matter (DOM) in these ecosystems is still scarce and unconnected (Mariot et al., 2007; Butturini et al., 2020; Boros et al., 2020; Jiang et al., 2022), despite it being an indispensable source of carbon and energy for the abundant heterotrophic bacteria occurring in these habitats (Lee et al., 2018) and probably an important component for explaining anomalous methane production measured in a productive saline-soda lake (Fazi et al., 2021). Consequently, determining the dynamic of the DOM in these ecosystems is a fundamental step in understanding how microbiota proliferate in these harsh habitats and the relevance of the carbon cycle in these ecosystems.

The abundance and quality of DOM in aquatic ecosystems are the result of an intricate balance between terrestrial allochthonous inputs (Da Silva et al., 2021), autochthonous biotic releases (Morling et al., 2017a), heterotrophic consumption (Morling et al., 2017b) and photodegradation (Gonsior et al., 2013; Herzsprung et al., 2020). Research on DOM in endorheic saline waters typically focus on the variability in the quality of DOM across water bodies at the regional scale (Wen et al., 2018; Song et al., 2019; Xu et al., 2020; Jiang et al., 2022) or among water layers in stratified lakes (Butturini et al., 2020). However, knowledge about temporal changes of DOM quality is still scarce (Jiang et al., 2022). Shallow H-SEAS are extremely dynamic in terms of hydrology and water salinity, which dramatically increases when the surface water evaporates. Therefore, only temporal monitoring can capture the dynamics and magnitude of these changes and determine their relevance in shaping the quantity and qualitative properties of DOM in these systems.

The fate of DOM during a hydrological transition from wet to dry conditions in H-SEAS can reflect the superposition of complex processes. On the one hand, during drying, water evaporation should cause a sharp rise in the DOM concentration in the water column. On the other hand, the increase in salinity during dry conditions is expected to reduce the solubility of some organic solutes (the salting-out phenomenon; Xie et al., 1997), especially proteinaceous (Li et al., 2012) and amphiphilic compounds (Lechtenfeld et al., 2013). Accordingly, the concentrations of some DOM moieties might decrease under high salinities. Simultaneously, the lack of interception of solar radiation by terrestrial vegetation should facilitate the photodegradation of aromatic fractions (Del Vecchio and Blough, 2006). Finally, the increase in temperature associated with drying might promote the growth of benthic and pelagic microbiota, consequently increasing the release/uptake of organic solutes. All together, these *in-situ* processes are expected to have a discernible influence on DOM properties and its potential bioavailability for heterotrophic microbiota or its photoreactivity. For instance, increased osmotic pressure in salt-saturated waters (i.e., brines, with salinities $>$ 30%) might lead to the release of osmoregulatory compounds by the microbiota or cell lysis, resulting in the exudation and hydrolysis of organic moieties from stressed halotolerant organisms (Altendorf et al., 2009). Therefore, an accumulation of fresh and saturated autochthonous compounds might be expected at high salinities. Furthermore, if the solubility of proteinaceous moieties decreases at high salinities, the C/N ratio is expected to increase. However, the opposite is expected if the DOM is absorbed onto the salt precipitates as a consequence of salt oversaturation (Li et al., 2012).

Finally, the ecological context of the surrounding area also matters. Shallow H-SEAS are typically located in flat and arid zones, with very little littoral and terrestrial vegetation and no canopy (Conesa Mor et al., 2011). Therefore, allochthonous inputs are expected to be small and sporadic, but might be relevant at certain times, especially during storm episodes.

In this context, the three main objectives of this study were to:

1 Determine the mass balance of dissolved organic carbon (DOC) in the water column during the transition from wet to dry conditions in an extremely dynamic H-SEAS to discern the impact of evaporation on *in-situ* DOC consumption/release.
2 Detail the synchrony/asynchrony of the DOC concentration based on its qualitative (e.g., spectroscopic) properties during the wet-to-dry transition.
3 Explore if and how the molecular chemo-diversity of the DOM changes as dryness and salinity increase.

To address these objectives, water samples were collected from a shallow H-SEAS in the Monegros Desert (NE Spain) for almost one year during a hydrological wetting-drying-rewetting transition. Furthermore, DOM from interstitial waters collected during the summer was analyzed, as well as that from a sample of salt crust that precipitated in the summer. Salts are a highly reflective material (surface albedo over 40% according to Craft and Horel 2019). Consequently, the impact of photodegradation on DOM accumulation within the salt crust and interstitial waters is expected to be small.

The qualitative characterization of DOM was performed with optical spectroscopy (absorbance and fluorescence), stoichiometry (the molar C/N ratio) and Fourier-transform ion cyclotron resonance mass spectrometry (FT-ICR-MS).

2. Material & methods

2.1. Study site

This study focused on La Salineta, a hypersaline shallow playa-lake (41°28′53″N, 0° 9′32″O) that covers a depression of 0.15 km^2. La Salineta is one of the numerous saline shallow lakes in karsic depressions in the Monegros Desert (Huesca-Zaragoza), locally called *saladas* (Conesa et al., 2011) (Fig. 1). This area in northeast Spain is a warm semi-arid region according to the Koppen-Geiger classification (Rubel and Kottek, 2010), with an extreme water deficit and a mean annual precipitation and evapotransporation of 350 mm and 1225 mm, respectively (Domínguez-Beisiegel et al., 2013). These shallow depressions originated from the dissolution of limestone, gypsum, and lutites and evaporitic materials (Salvany et al., 1995). These lagoons are surrounded by flat dry agricultural lands and not impacted by industrial activities. In comparison to the nearby shallow saline lakes, La Salineta shows the longest wet cycle (Castañeda and Herrero, 2005). When flooded the water column is typically 20–30 cm depth. In contrast, in the summer, the water column is simply a thin layer (1–2 cm in depth) of brine that rests on the salt crust (3–5 cm thick), due to the proximity of a permanent water table. In the summer, the salt crust covers approximately 60% of the total lake bed and is mainly composed of halite (84.2%) and bloedite ($Na_2Mg(SO_4)_2 \times 4H_2O$, 15.1%), with a small amount of calcite (0.7%; Appendix SI1). Particulate organic matter in the salt crust averages 9 ± 3 gC/m^2. In the water column, the pH typically ranges from 7.5 to 8.8, while the oxide reduction potential (ORP) varies from 330 to −175 mV, with the lowest values occurring in brines.

Chlorophyll concentration in the water column ranged between 2.4 and 230 mg/L. Being the high value the highest in comparison to that of the other nearby H-SEAS (Menendez-Serra et al., 2020), while the density of planktonic prokaryotes ranges between 9×10^5 and 8×10^7 cells ml^{-1} (unpublished data from the authors).

2.2. Field sampling

La Salineta was sampled from January to December 2020. Sampling started January 28th under extremely wet conditions due to the occurrence of Storm Gloria a few days earlier. Water samples were collected from the surface on seven dates (28/01, 21/05, 15/06, 30/06, 20/07, 09/10 and 29/12) and interstitial waters on four dates- (30/06, 20/07, 09/10 and 29/12). Surface waters with salinity higher than 30% were

Fig. 1. Areal image of la Salineta under dry conditions (May 2019, Images from Google Earth). Red oval indicates the sampling area. The upper left inset a map of Spain and the location (black circle) of the study site. The upper right picture shows an image of the lagoon in summer 2020.

defined as brines. In addition, DOM was analyzed from a sample of salt crust that had precipitated on the playa lake bed in the summer.

On each sampling date, 0.5 L of surface water were filtered in the field with precombusted GF/F glass fiber filters (Whatman). An aliquot (250 ml) was acidified to pH 2 with an HCl solution. All samples, acidified or not, were stored at 4 °C prior to analysis. Waters with salinities higher than 20% were diluted to 10% to avoid salt precipitation. Interstitial waters were collected at a depth of 20 cm from sediments using four tensiometers equipped with a ceramic suction cup (Irrometer, model SSAT). Tensiometers were inserted into the sediments for 3–4 h before water collection. A few milliliters of water were typically collected with each tensiometer. Therefore, all the samples were merged into one larger sample of 80–120 ml. The sample was then filtered in the field with precombusted GF/F glass fiber filters and acidfied to pH 2.

A plate of salt crust measuring approximately 0.05 m^2 and 3 cm thick was collected in the summer and transported to the laboratory under dark conditions at 4 °C. In the laboratory, the salt crust was dissolved in 2 L of ultrapure water and filtered with precombusted GF/F glass fiber filters. The resulting solution was acidified to pH 2 and stored at 4 °C prior to analysis. The salinity of the surface and interstitial waters was measured *in situ* with a refractometer (HRS"8-T, Kruss, Germany).

2.3. Environmental descriptors

The temperatures of surface waters and in interstitial saturated sediments were monitored continuously with Hobo Pendant MX water temperature data loggers. Sensors were installed in January at the lake edge and inserted into sediments at a depth of 10 cm. The sensor submerged in the water column leaned on the lake bed and remained out of the water from June 15th 2020 to November 5th 2020 as a consequence of the surface water contraction.

This interval could be identified by the Hobo temperature sensor recording anomalous large daily temperature oscillations, revealing that the sensor was out of the water and measuring the temperature of the air in contact with the salt crust (Fig. 2c).

Pluviometry and daily air temperature data were obtained from a meteorological station located at the Zaragoza airport (65 km away from the sampling site) and managed by the Agencia Española de Meteeología (AEMET, www.aemet.es). Variations in the surface water of La Salineta were monitored during the study period using Sentinel Playground, which provides satellite images that are refreshed every 7–10 days.

2.4. Biogeochemical analysis

Dissolved organic carbon (DOC) content and total dissolved nitrogen (TDN) levels in water samples were measured with the multi N/C 3100 analyzer (Analytik Jena) (detection limit is 0.1 mg L^{-1}). All samples were diluted 1/5–1/20 to minimize the impact of the salts on instrument performance. Dissolved organic nitrogen (DON) content was analyzed by subtracting the amount of dissolved inorganic nitrogen (DIN) from that of TDN.

DIN content was determined with colorimetric methods: nitrate + nitrite was estimated with a Bran + Luebbe autoanalyzer equipped with a reductive copper cadmium column (detection limit: 50 mg L^{-1}). Ammonium levels were estimated with the salicylate method of Reardon (1969) (detection limit: 25 mg L^{-1}). To minimize interference from the salts and sulfite, all samples were diluted 1/5–1/10 with ultrapure Milli-Q water.

To measure the impact of Storm Gloria on the input of new water into La Salineta, dD and $d^{18}O$ of the water samples were measured by pyrolysis using a Thermo-Quest high-temperature conversion elemental analyzer (TC/EA) unit with a Finnigan MAT Delta XP IRMS. The results are expressed in terms of δ relative to international standards (V-SMOW for δ^2H-H_2O and $\delta^{18}O$-H_2O).

The major metals (Ca, Na, S, Mg and K) were analyzed with inductively coupled plasma optical emission spectrometry (ICP-OES, Optima 3500, PerkinElmer, Waltham, USA) and inductively coupled plasma mass spectrometry (ICP-MS, nexION 350, PerkinElmer, Waltham, USA). All samples were diluted 1/20–1/50. Dilutions precluded the detection

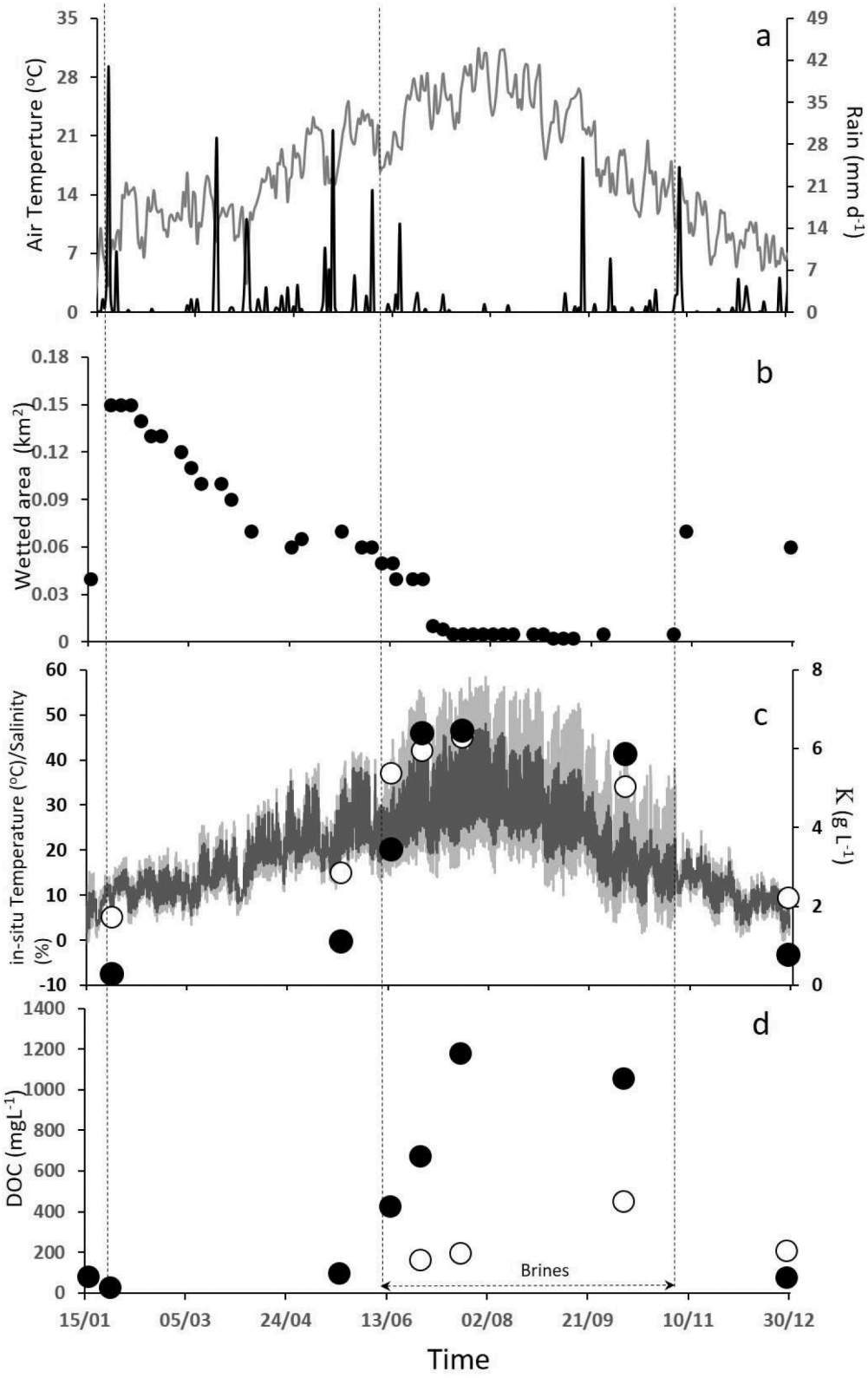

Fig. 2. Hydroclimatic and biogeochemical context in La Salineta during the study period. (a) Air temperature (gray line) and daily precipitation (black line) in Zaragoza (65 km from the study area). (b) Surface of the wetted area of La Salineta (information obtained from the Sentinel satellite). (c) *In-situ* temperatures recorded with the two Hobo sensors. The first one was located at the top of the salt crust of the playa (light gray line). The second one was inserted into the sediments at a depth of 10 cm (dark gray line). Salinity (open dots) and the K concentration (closed dots) recorded in the water column are shown. (d) DOC concentration in the surface (black dots) and interstitial waters (open dots) during the study period. The three vertical dashed lines (from left to right) indicate the timing of Storm Gloria, the formation of brines in the surface waters and the autumnal rewetting, respectively.

of more diluted metals such as Fe. The high solubility of potassium was used as a conservative tracer (Lopez and Mandado, 2007) to determine the DOC mass balance (see Section 2.5). In fact, in contrast to halite, bloedite and calcite (salts not bearing potassium), sylvite (potassium salt) did not achieve the saturation threshold during the study period (Appendix SI2) and was also missing in the salt crust (SI1 and Esther Sanz-Montero, personal communication).

Qualitative characterization of the DOM was performed using a combination of three analytical approaches:

(a) Spectroscopy: absorbance and fluorescence.
(b) Stoichiometry: estimating the molar C/N ratio

(c) Fourier-transform ion cyclotron resonance mass spectrometry (FT-ICR-MS)

2.4.1. Spectroscopy and the C/N ratio

Due to the extremely high DOC values in brines during the summer and the large differences in DOC concentrations among samples (see the Results section), all acidified samples were diluted to a final DOC concentration of 5–10 mg/L and to a final salinity ranging from 0.5 to 1.5% to mitigate the interference from the inner filter effect during the spectroscopy measurements.

Samples were maintained at room temperature and filtered with 0.2-mm nylon filters prior to analysis.

The UV1700 Pharmaspec spectrophotometer (Shimadzu, Japan) was used to obtain absorbance spectra. Data were obtained in the double-beam mode, with the wavelength scanned from 200 to 600 nm (the slit width was set to 1 nm). Deionized water with 1% salinity was used as the blank.

Absorbance spectra were used to estimate the specific aromaticity at 254 nm ($SUVA_{254}$) and the spectral slope between 275 and 295 nm ($S_{275–295}$). $SUVA_{254}$ was estimated according to the method of Weishaar et al. (2003). $S_{275–295}$ was estimated by fitting the log-transformed absorption spectra obtained between 275 and 295 nm. $S_{275–295}$ values typically increase upon irradiation and inversely correlate with the molecular weight of the DOM (Helms et al., 2008).

Fluorescence spectra were obtained with an RF-5301 PC spectrofluorometer (Shimadzu, Japan) equipped with a xenon lamp and a light-source compensation system (S/R mode). For each sample, a three-dimensional excitation-emission matrix (EEM) was obtained. Each EEM consisted of 21 synchronous scans with 1-nm increments both in emission and in excitation. The excitation wavelength ranged from 250 to 410 nm, with intervals of 10 nm. The emission wavelength ranged from 310 to 530 nm, with intervals of 10 nm. The bandwidth used for both excitation and emission was 5 nm. A 1-cm quartz cell was used to perform the measurements.

Each EEM was corrected and normalized following the steps described by Goletz et al. (2011). The excitation correction function was determined using rhodamine B as a quantum counter (Lakowicz, 2006), whereas the emission correction was obtained by comparing the reference spectra of quinine sulfate and tryptophan provided by the National Institute of Standards and Technology (NIST) (Gardecki and Maroncelli, 1998). Data were normalized by the area under the Raman peak obtained for an ultrapure MQ water sample at {λex350 nm, λem371–428 nm} (Lawaetz and Stedmon, 2009). The inner filter effect was corrected by comparing absorbance measurements (Larsson et al., 2007; Lakowicz, 2006).

EEM spectra were used to estimate three DOM qualitative proxies: the fluorescence index (FI), the biological index (BIX) and the humification index (HIX). The FI positively correlates with the accumulation of microbial-derived DOM relative to terrestrial inputs (McKnight et al., 2001). It is the ratio of the fluorescence intensity emitted at 470 nm to that at 520 nm at an excitation wavelength of 370 nm. BIX values positively correlate with the accumulation of recent autochthonous DOM. It is the ratio of the fluorescence intensity emitted at 380 nm to that at 430 nm at an excitation wavelength of 310 nm (Huguet et al., 2009). The HIX is a proxy for the amount of humic substances. Higher values indicate a higher humification degree (Ohno, 2002). It is calculated by dividing the area of the emission spectra between 435 and 480 nm by the sum of the areas of the emission spectra between 435 and 480 nm and between 300 and 345 nm at an excitation wavelength of 254 nm.

The molar C/N ratio of the DOM was calculated after estimating the molar concentrations of DOC and DON.

2.4.2. SPE extraction and FT-ICR-MS

The solid-phase extraction (SPE) of DOM (SPE-DOM) was performed in all the samples. The SPE-DOM recovery efficiency averaged 36.5% (Appendix SI3). However, the recovery rate of the Sup200720 sample (18.5%) remained outside the interquartile range. Therefore, the results from this sample were removed from the data analysis (Appendix SI4). Filtered acidified samples were concentrated through 100-mg styrene-divinylbenzene-polymer type (PPL) solid-phase cartridges (Agilent, Technologies, Santa Clara, CA, United States), according to the protocol described by Dittmar et al. (2008). SPE-DOM extracts were diluted 1:1 (v/v) with ultrapure water and analyzed with an FT-ICR-MS equipped with a dynamically harmonized analyzer cell (solariX XR, Bruker Daltonics Inc., Billerica, MA) and a 12 T refrigerated actively shielded superconducting magnet (Bruker Biospin, Wissembourg, France). The instrument is located at the ProVIS center for Chemical Microscopy within the Helmholtz center for Environmental Research (Germany). Samples were infused in random order by an autosampler at a flow rate of 10 μL min^{-1} and measured with negative mode electrospray ionization (Apollo II ESI source, capillary voltage = 4.2 kV). For each spectrum, 256 scans (ion accumulation time = 15 ms) were co-added in the mass range 150–3000 *m/z*, with a 4-MWord time domain in absorption mode (Da Silva et al., 2020). Mass spectra were internally calibrated with a list of peaks (*m/z* 250–550, $n > 110$) commonly present in natural organic matter. Mass accuracy after an internal linear calibration was better than 0.1 ppm. Peaks were considered if the signal/noise (S/N) ratio was greater than four.

Formulae were assigned to the peaks in the mass range 150–700 *m/z*, allowing for elemental compositions $C_{1–60}H_{1-120}O_{1–40}N_{0–4}S_{0–1}$ with an error range of ± 0.5 ppm, according to Lechtenfeld et al. (2015). Relative peak intensities were calculated based on the summed intensities of all the assigned peaks in each sample. The molecular formula of a mass peak is referred to as "molecule" in this article although one molecular formula can represent several or even millions of different structural isomers. Only formulas with $-10 \leq DBE - O \leq +10$ (DBE: double bound equivalents) were considered for further data evaluation (Herzsprung et al., 2014).

After molecular formula assignement, the following molecular descriptors were calculated: the number of detected molecules (richness) and intensity-weighted averages of molecular mass; the H/C, O/C and C/N ratios; double bound equivalent (DBE), modified aromaticity index (AI_{mod}; Koch and Dittmar, 2016) and nominal oxidation state of carbon (NOSC, LaRowe and Van Cappellen, 2011); and the CHO, CHNO, CHNOS and CHOS molecular classes.

The H/C ratio, DBE and AI_{mod} provide information about the degree of saturation of a molecule (i.e., the number of C = C double bounds), whereas the O/C ratio and NOSC are descriptors of the (average) carbon oxidation state. According to the values of the different DOM indicators, the DOM molecular classes were split into: carboxyl-rich alicyclic like molecules (CRAM), aliphatic-like substances, aromatic-like compounds, condensed and aromatic-like substances (CA) and highly oxygenated molecules. Criteria adopted to constrain the molecular classes are detailed in Appendix SI5). Each formula can describe numerous isomers; therefore, this classification suggests the most likely structure (Rossel et al., 2017).

2.5. Data analysis and statistics

A DOC mass balance was determined to discern the impact of evaporation from *in-situ* processes on DOC concentration. Potassium concentrations were used as conservative tracers to estimate the expected DOC concentration during the study period. Estimates were performed according to the following formula:

$$[DOC]_{e(t)} = \frac{[DOC]_{m(0)}}{[K]_{(0)}}[K]_{(t)} \quad (1)$$

where $[DOC]_{e(t)}$ describes the expected values of DOC concentration at each sampling time *t*, $[DOC]_{m(0)}$ is the measured value of DOC at time 0, and $[K]_{(t)}$ and $[K]_{(0)}$ are the measured concentrations of potassium at

each sampling time *t* and at time 0, respectively. Time 0 corresponds to the sampling performed right after Storm Gloria when La Salineta was under extreme wet conditions.

Comparison between the measured and expected values of [*DOC*] was used to determine the following net balance:

$$\text{if}: [DOC]_{e(t)} = \left\{ \begin{array}{c} > [DOC]_{m(t)} \ indicates\ a\ net\ in-situ\ depletion\ of\ DOC \\ = [DOC]_{m(t)} \ indicates\ that\ evaporation\ drives\ the\ amount\ of\ DOC \\ < [DOC]_{m(t)} \ indicates\ a\ net\ in-situ\ release\ of\ DOC \end{array} \right\} \quad (2)$$

The synchrony between changes in the DOC concentration and DOM qualitative proxies was explored by visualizing the relationships of the DOM proxies with the DOC plots. The shape, hysteresis and rotational pattern of these plots provide a rapid indication of the strength and non-linearity of the coupling (Butturini et al., 2008).

Correlations between variables were assumed to be statistically significant at $p < 0.05$.

Paired *t*-test was used to evaluate differences in the DOM optical descriptors between brines and interstitial waters (both collected exclusively in the summer). Differences were assumed to be statistically significant at $p < 0.05$.

Differences in the FT-ICR-MS elemental formula among the samples were tested with a hierarchical cluster analysis (HCA). The analysis included the 2914 molecules detected in all the samples after ranking the SPE-DOM mass peak intensities for each of the eleven samples separately. Squared Euclidean distances with Ward's linkage were applied (Murtagh and Legendre, 2014) by assigning first rank to the variable with the highest intensity.

Visualization of the qualitative differences of SPE-DOM involved the use of van Krevelen diagrams from an inter-sample ranking analysis (Herzsprung et al., 2017)

For each SPE-DOM molecular class and descriptor, the weighted average was estimated from the relative intensity of the peak of each assigned molecule.

Rank correlation analysis was performed with components that were present in 10 of the 11 samples (6 surface water samples + 4 interstitial water samples + 1 salt crust leachate). The ranks of mass peak intensities were calculated for each of the 10 samples. The inter-sample ranks were calculated from the intensity ranks as explained by Herzsprung et al. (2017). The inter-sample ranks were correlated with the DOC concentration ranks for each of the 2914 formulas, using Spearman's rank correlation as described earlier (Herzsprung et al., 2012). The rank correlation coefficients and corresponding p-values are listed in the appendix excel file "ALLMolecule_RankAnalysis_SupWater_Spearman Results.xls".

3. Results

3.1. Climatic, hydrological and geochemical context

Storm Gloria caused the total flooding of the La Salineta shallow lake. After that, the wetted area of the lake gradually contracted at a rate of approximately 945 m^2 d^{-1}, with transient rises in April-May 2020 after a few rain episodes (Fig. 2a, b). Evaporation accelerated in late June and a shallow (< 3 cm in depth) brine layer was constrained to the more depressed part of the shallow lake (approximately 5000 m^2). In short, 97% of the flooded playa had disappeared in 5 months. Brines persisted throughout the summer and up to the middle of November, when an autumnal rain episode reflooded 50% of the depression (Fig. 2b). In the summer, the temperature of the air in contact with the salt crust showed daily oscillations within the range of 35 °C, with 20 °C and 55 °C being the lowest and highest values, respectively. In the shallow sediments, the daily temperature oscillations were of 20 °C, with the highest temperatures rarely exceeding 45 °C (Fig. 2c).

Right after Storm Gloria, the $d^{18}O$ and dD values measured in the waters from La Salineta were identical to the long-term weighted $\delta^{18}O$ and dD values recorded for the precipitation in Zaragoza (Araguas-Araguas and Teijeiro, 2005), indicating that the playa was totally flooded by new rain water. Evaporation strongly intensified the fractionation of the two isotopes. Consequently, the $d^{18}O$ and dD values showed a strong deviation from meteoric water lines. Autumnal rewetting affected the input of new water. However, the $d^{18}O$ and dD values showed little deviation from meteoric water lines, revealing that the "new water" from the rain had mixed with the residual "old water" from the brines and that the rain episodes were far from being comparable to Storm Gloria (Appendix SI6).

Salinity (and the main metals, Appendix SI7) and water temperature were significantly correlated ($r = 0.89$, g.f. = 5, $p < 0.05$). The increase in water temperature (late spring-early summer) preceded that of salinity and dissolved salt concentrations. After Storm Gloria, under wet conditions, salinity in La Salineta (5.1%) was a little higher than that of marine waters. After that, salinity increased progressively up to 34–45% in June-October. In December, after the autumnal rewetting, salinity returned to 9%. Interstitial waters were sampled during the driest period only. The salinity of interstitial waters (32 ± 2.5%) was slightly lower than that of brines (39 ± 5%), but this difference was not statistically significant ($t_{paired} = 2.27$; $p > 0.05$).

3.2. DOC dynamics and mass balance

DOC concentration in the water column ranged from 28 to 1174 mg/L, correlating significantly with salinity ($r = 0.86$, d.f. = 5, $p < 0.01$) but not with temperature ($r = 0.65$, d.f. = 5, n.s.). Although the DOC peak concentration coincided with that of temperature and salinity, its pulse began with a time delay with respect to the environmental variables (Fig. 3). The DOC level in interstitial waters (225 ± 113 mg/L) was significantly lower than that in surface waters collected during the same period (842 ± 340 mg/L, $t_{paired} = 4.56$, $p < 0.05$, Fig. 2d).

The DOC mass balance obtained from the potassium concentrations revealed that DOC behaved nearly conservatively during wet conditions (i.e., May and December). However, in June and, more remarkably, in July-October, a net release of DOC was estimated. During the driest conditions (July-October), the measured DOC content was almost double the expected concentration (Fig. 3).

3.3. DOM optical qualitative descriptors

As a whole, spectroscopic analysis revealed that the DOM from La Salineta showed remarkably low aromaticity (low $SUVA_{254}$ values), a low humification degree (low HIX values), and an accumulation of

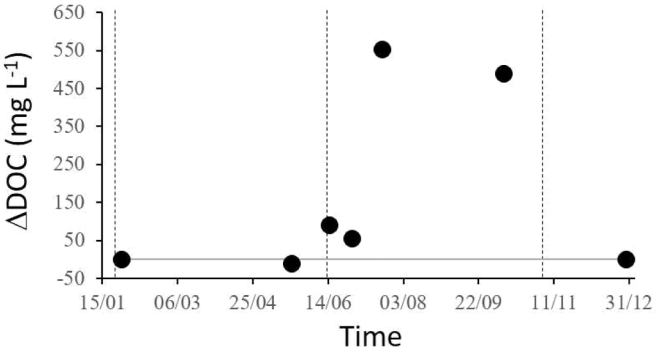

Fig. 3. Temporal dynamics of the estimated net balance of DOC obtained from the potassium values. Positive values indicate a net DOC accumulation, while negative values indicate the opposite. The three vertical dashed lines (from left to right) indicate the timing of Storm Gloria, the formation of brines and rewetting, respectively. The gray horizontal line indicates that DOC = 0.

small-sized moieties (large $S_{250–275}$ values) and fresh organics of an autochthonous origin (large BIX values) when the values were compared to those of typical freshwater ecosystems (Appendix SI8).

EEMs showed classic bimodal features, with the largest peaks corresponding to humic and fulvic-like fluorophores (Fig. 4, Chen et al., 2003). However, the fulvic peak was strongly attenuated for the DOM obtained from the salt crust (Fig. 4e). Comparing the shape of the EEM of the sample collected under wet conditions (January) with that of the brine (July), a depletion in the fluorophore signal typically assigned to protein-like substances (B, T peaks) and an increase in fluorescence in the region of the spectrum close to that corresponding to marine humic-like fluorophores (M peak) were observed for the brine sample (Fig. 4c). On the other hand, the EEM of the salt crust leachate showed the strongest signal for the tryptophan-like fluorophore (peak T, Fig. 4e).

The optical descriptors of DOM (i.e., $SUVA_{254}$, E2:E3, BIX, HIX and FI) were not significantly different between the interstitial waters and brines (paired *t*-test, all t values < 2.1, $p > 0.05$). However, DOM from interstitial waters tended to be slightly more humified, aromatic, larger in relative size and degraded compared to that of surface water (Table 1).

DOM from the salt crust sample was richer in aromatic (larger $SUVA_{254}$ values) and microbial-like moieties (larger FI) compared to that from brines (Table 1).

Regarding the surface waters, almost all the DOM descriptors showed remarkable fluctuations during the study period. However, only $S_{275–295}$ significantly (positively) correlated with an environmental parameter (i.e., with salinity, $p < 0.05$).

When the changes in the quality proxies for DOM were compared to those of the DOC content, three main responses were observed:

(a) The most important one included three DOM parameters ($S_{275–295}$, FI and the C/N ratio), whose highest values preceded that of the DOC concentration peaks. Therefore, their relationships with DOC concentration were non-linear and with a clockwise hysteresis pattern (Fig. 5a), revealing that these parameters increased faster than the DOC content (Fig. 4a).

(b) The BIX parameter (Fig. 5b) showed an abrupt increase in May, remained almost steady during the driest period and showed a final increase coinciding with the autumnal rewetting. Hence, the BIX-DOC relationship showed a counter-clock loop (Fig. 4b).

(c) $SUVA_{254}$ and the HIX abruptly decreased in May, but remained almost steady thereafter for the rest of the study period (Fig. 5c).

3.4. FT-ICR-MS of SPE-DOM

A total of 9415 distinct molecular formulas (MFs) was detected by FT-ICR-MS. The number of MFs in each sample ranged from 4028 to 5830. The six samples from surface waters (brines included) shared 3449 MFs. Weighted average masses of all the samples ranged from 354 to 370 *m/z*, with larger values observed for the surface waters.

The HCA grouped the samples into two main clusters: one cluster comprised the interstitial waters and brines, while the other included the three surface water samples with lower salinity and, interestingly, the salt crust leachate (Fig. 6. For a visualization of the Van Krevelen diagrams see Appendix SI9).

Overall, the most abundant group in SPE-DOM was CRAM-like substances (46–52% of the relative peak intensity) followed by the aliphatic-like group (between 5.8 and 19.5%) and aromatic-like group (1.5–3.4%). By contrast, CA represented less than 0.5%. SPE-DOM from the salt crust sample stood out for having the lowest percentage of CRAM–like molecules and the highest percentage of aliphatic-like groups. SPE-DOM from surface and interstitial waters showed similar compositions; however, interstitial waters tended to have a more aromatic and unsaturated molecules (higher AI_{mod} and DBE) and fewer aliphatic substances. The C/N ratio ranged between 29 and 50, being the lowest for the salt crust SPE-DOM (Table 2, more details at Appendix SI10), suggesting a selective accumulation of nitrogen-bearing molecules in the salt crust.

In the surface waters, the relative contribution of the compositional groups changed during the study period (Fig. 7). After Storm Gloria, SPE-DOM was rich in CRAM-like molecules, with a moderate-high level of aromaticity and unsaturation (high AI_{mod} and DBE, respectively) and

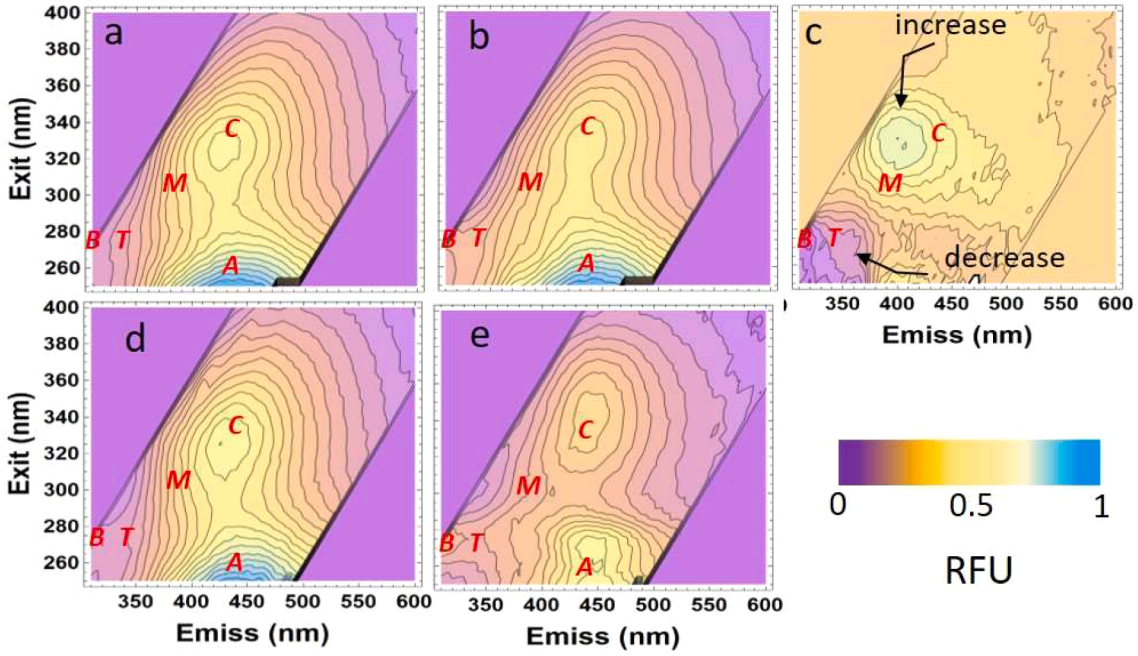

Fig. 4. EEMs of DOM from La Salineta in the water column under wet conditions (January, panel *a*) and brines (July, panel *b*), as well as in interstitial waters (July, panel *d*) and the salt crust leachate (panel *e*). Panel *c* shows the difference between panel *b* and *a*. Arrows in panel *c* indicate the regions in the EEM of brines that increased or decreased with respect to those in the EEM of the sample obtained under wet conditions. Red letters in the panels show the position of the peaks corresponding to fluorophores typically detected in waters. *B* and *T*: tyrosine and tryptophan-like fluorophores; *M*: marine humic-like compounds; *C*: humic-like substances; *A*: fulvic-like substances (Chen et al., 2003). Colours of contour plots are proportional to the relative fluorescence intensity unit (RFU).

Table 1
DOC (in mg L^{-1}) and the average values of the optical descriptors of DOM (± SD) obtained for each water sample. In all cases, $n = 3$, except for interstitial waters and the salt crust leachate. SD = ± 0 indicates an SD < 10^{-4}. "Sup": surface waters; "Int": interstitial waters. Surface water samples collected from July 15th to October 9th correspond to brines. Units of $SUVA_{254}$ are L mgC^{-1} m^{-1}.

Sample	DOC	C/N	FI	HIX	BIX	$S_{275-295}$	E2:E3	$SUVA_{254}$
Salt crust leacheate	0.1** (NA)	17 (NA)	1.81 (NA)	0.8 (NA)	0.73 (NA)	0.031 (NA)	32.6 (NA)	2.59 (NA)
Sup28/01	26 (± 2)	16.1 (± 1.7)	1.49 (± 0)	0.91 (± 0.05)	0.61 (± 0.12)	0.025 (± 0.002)	9.1 (± 2.7)	2.4 (± 0.17)
Sup21/05	95 (± 6)	27.3 (± 5.5)	1.48 (± 0.01)	0.86 (± 0.01)	0.71 (± 0)	0.035 (± 0)	16.1 (± 1.4)	1.8 (± 0.12)
Sup15/06	422 (± 21)	23 (± 4.3)	1.53 (± 0.01)	0.8 (± 0.01)	0.71 (± 0)	0.04 (± 0.003)	38.4 (± 18.3)	0.45 (± 0.02)
Sup30/06	670 (± 15)	26.4 (± 2.5)	1.58 (± 0.07)	0.78 (± 0.02)	0.69 (± 0)	0.04 (± 0)	25.8 (± 12.4)	1.04 (± 0.22)
Sup20/07	1174 (± 64)	20.4 (± 1.5)	1.52 (± 0.01)	0.81 (± 0.02)	0.71 (± 0)	0.039 (± 0.003)	27.7 (± 6.1)	0.82 (± 0.02)
Sup09/10	1051 (± 71)	18.2 (± 1.3)	1.53 (± 0.01)	0.79 (± 0.01)	0.75 (± 0.01)	0.04 (± 0.003)	17.2 (± 3.1)	1.03 (± 0.03)
Sup29/12	74 (± 6)	23.5 (± 3.1)	1.46 (± 0.02)	0.81 (± 0)	0.79 (± 0)	0.033 (± 0)	18.3 (± 0)	0.73 (± 0)
Int30/06	159 (NA)	12.1 (NA)	1.46 (NA)	0.86 (NA)	0.62 (NA)	0.033 (NA)	28 (NA)	2.34 (NA)
Int20/07	193 (NA)	16.6 (NA)	1.50 (NA)	0.77 (NA)	0.72 (NA)	0.036 (NA)	20.8 (NA)	1.01 (NA)
Int09/10	447 (NA)	19.6 (NA)	1.57 (NA)	0.82 (0)	0.7 (NA)	0.04 (NA)	18.3 (NA)	1.15 (NA)
Int29/12	207 (NA)	NA	1.39 (NA)	0.87 (NA)	0.61 (NA)	0.025 (NA)	15.1 (NA)	2.34 (NA)

** for the salt crust leachate, the DOC value is presented as gC/m^2 of the salt crust.

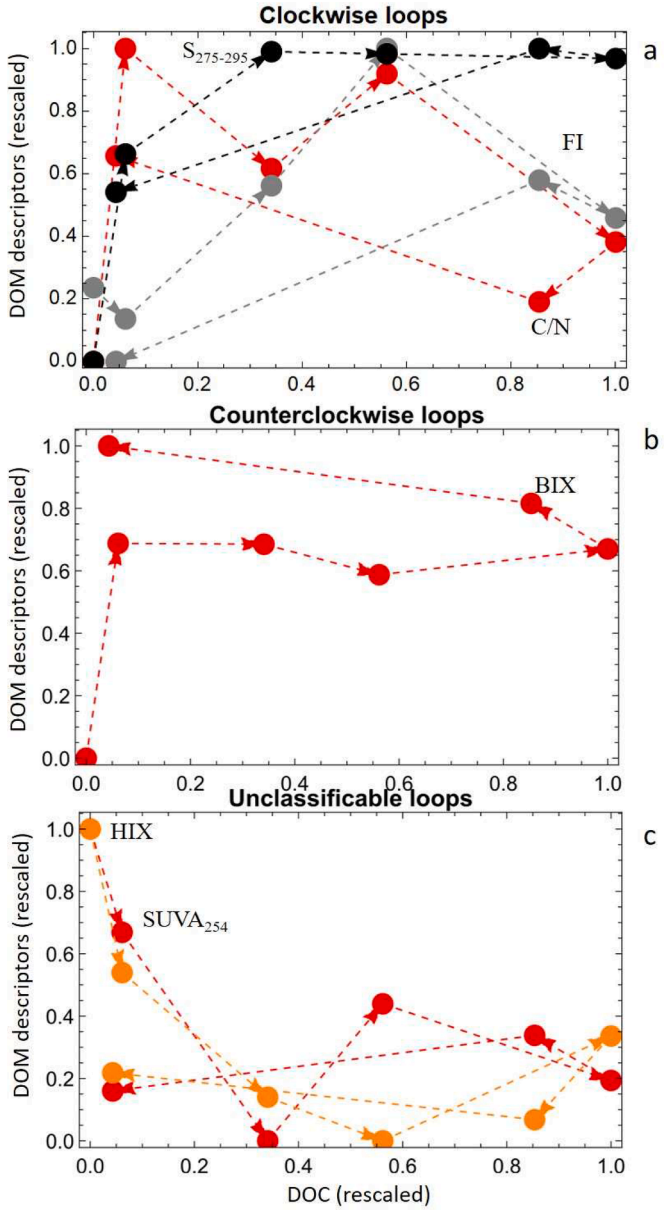

Fig. 5. Relationships between the qualitative parameters of DOM vs the DOC content. Arrows indicate the temporal succession. The three plots show the main responses. All parameters were rescaled between 0 and 1.

a low carbon oxidation state (i.e., low NOSC). In May, under moderate salinity and DOC concentration, the NOSC remained almost constant, but both the AI_{mod} and DBE decreased substantially. Furthermore, the relative contribution of CRAM–like molecules decreased strongly, while the contribution of aliphatic-like molecules slightly increased. Under increased salinity and DOC concentration (i.e., brines), SPE-DOM quality shifted towards a higher oxidation state, while neither aromaticity nor the saturation degree changed substantially. The contributions of CRAM-like and aliphatic–like molecules decreased, while a substantial increase in highly oxygenated molecules was detected. Finally, during the autumnal rewetting, SPE-DOM showed low aromaticity (low AI_{mod}), more saturation (low DBE) and less oxidation (low NOSC). The relative contributions of CRAM-like and aliphatic-like molecules increased again, while that of the highly oxygenated molecules returned to low values. Remarkably, the relative intensities of the highly oxygenated moieties strongly covaried with the DOC content during the entire study period ($r = 0.98$, d.f. $= 4$, $p < 0.001$, Fig. 7b).

Molecular changes under high DOC-salinity conditions were visualized with the Spearman's rank correlation analysis. Fig. 8a shows that almost 30% of the MFs significantly correlated with the DOC concentration ($p < 0.05$). Of these, 14% correlated positively with DOC, while the rest were correlated negatively. These two groups were clearly separated along the O/C ratio axis, with the MFs positively correlating with the DOC concentration showing an O/C ratio larger than 0.5. Furthermore, the MFs positively correlating with the DOC concentration were typically smaller than 450 *m/z*. By contrast, there were no trends observed in the mass of the MFs negatively correlating with the DOC level (Fig. 8b).

A positive correlation between the relative contribution of nitrogen-bearing molecules and the DOC concentration was also observed ($r = 0.875$, g.l. $= 4$, $p < 0.025$). For example, 62% of the MFs that accumulated at high DOC levels according to the Spearman's rank correlation contained nitrogen. This percentage decreased to 22% for the molecules that decreased in abundance at high DOC levels.

SPE-DOM collected just after Storm Gloria and that collected after the autumnal rewetting showed clearly different signatures. The sample collected after Storm Gloria had more aromatic and more unsaturated molecules, but only few aliphatic-like molecules. By contrast, the SPE-DOM collected during rewetting shared several similarities with that obtained from the salt crust: low values of NOSC, AI_{mod} and DBE, as well as a high relative contribution of aliphatic-like compounds and a low relative contribution of highly oxygenated compounds (Fig. 7).

Non-oxygen heteroatom molecules CHNO, CHOS and CHNOS molecules accounted for the 18–25%, 13–18% and 2–4%, respectively of SPE-DOM total peak intensity (Table 2 and Appendix SI10). Larger relative intensities occurred in summer brines. Among heteroatom molecular categories, the most remarkable result was the accumulation of S-bearing highly oxygenated molecules with a peak relative signal

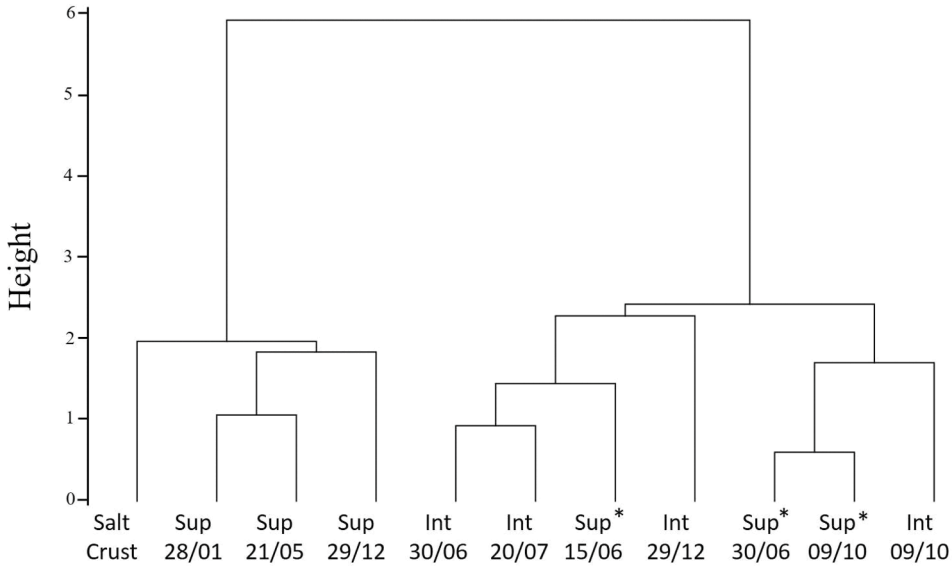

Fig. 6. HCA dendrogram of the eleven SPE-DOM samples analyzed with FT-ICR-MS. "Sup": surface waters; "Int": interstitial waters. * indicates brines (salinity > 30%) in surface waters. See SI7 for specific van Krevelen diagrams showing the inter sample rankings.

higher than that of CHO analogous molecules. In contrast, N-bearing highly oxygenated molecules did not showed such accumulation in brines (Appendix SI10).

Overall, heteroatom molecules were typically more oxidized and less aromatic (ie. higher NOSC and lower AI_{mod} and DBE values, respectively) than CHO ones

4. Discussion

The shallow lake of La Salineta is a highly dynamic system that undergoes large oscillations in salinity as a result of the alternation of wet and dry phases. This study highlighted how this dynamism alters the quantity and quality of DOM.

DOC levels increased by up to two orders of magnitude during the transition from wet conditions to brine formation. Such an increase is inconceivable in lotic systems and is much larger than that reported in other organic-rich saline systems in the world (Mariot et al., 2007; Osburn et al., 2011; Butturini et al., 2020). Although information from H-SEAS lakes worldwide is scarce and incomplete, these large oscillations in DOC content are probably a remarkable signature of these harsh systems. The mass balance in La Salineta revealed a large amount of DOC emerging with the formation of brines. Approximately 45% of this could not be attributed to evapoconcentration. This indicated an outstanding net *in-situ* production that could not be counterbalanced by photooxidation, the reduction in solubility of DOM molecules at high salinities or by heterotrophic consumption.

The DOC increase detected in brines showed a time delay with respect to the increase in temperature and salinity. Previous studies have reported that La Salineta hosts a highly dynamic and diverse microbial planktonic community composed of bacteria, archaea, microeukaryotes and fungi, with heterotrophic prokaryotes and photoautotrophic eukaryotic Chlorophyta (*Dunaliella salina*) being predominant under high salinities (Menéndez-Serra et al., 2021). Prokaryotes and microeukaryotes that thrive in such oscillating and extreme salinity conditions synthesize and accumulate organic compounds as carbon reservoirs and osmolytes to counteract the external osmotic stress (i.e., a "salt out" osmoadaptation strategy, Menéndez-Serra et al., 2021). For instance, healthy and senescent *Dunaliella salina* excretes large amounts of glycerol and derivatives that, in turn, can support a high density of heterotrophic bacteria and archaea (Oren, 1993; Bardavid et al., 2008; Orellana et al., 2013). Therefore, the delayed increase in the DOC concentration might reflect a rising imbalance between the DOM mineralization caused by heterotrophic consumption and photodegradation and the DOM released by primary producers and any senescent/lysed cells under osmotic stress.

La Salineta and almost all of the hypersaline playa lakes in arid zones are totally unshaded and permanently irradiated by the sun. The impact of solar radiation on DOM is well recognized and has been comprehensively studied (Del Vecchio and Blough, 2006; Gonsior et al., 2013; Herzsprung et al., 2020). However, our results suggested that the effects of photodegradation on DOM appeared to be relevant at the beginning of the study period (January-May), based on the observed reductions in aromaticity (decreases in the $SUVA_{254}$ and AI_{mod}), the relative molecular size (increase of $S_{250–275}$) and the unsaturation degree (decrease in the DBE) (Helms et al., 2008; Vähätalo and Wetzel, 2008; Xu et al., 2020). DOM from interstitial waters and the salt crust leachate was slightly richer in aromatic descriptors ($SUVA_{254}$, aromatic-like and CA-like proxies), indicating that the effects of photodegradation must be minor in these cases (especially in interstitial waters).

Once brines were formed and the DOC concentration had increased, the relevance of photodegradation on DOM declined ($SUVA_{254}$, $S_{250–275}$, AI_{mod} and DBE remained almost constant in these samples). By contrast, the excess of DOC was coupled with an increase in autochthonous and fresh moieties (as suggested by the high values of the BIX and FI), reinforcing the suggestion that the DOC had originated from the microbiota, as described above. Simultaneously, FT-ICR-MS revealed the accumulation of oxidized molecules under the highest salinity and DOC concentrations. This shift was opposite to that expected if the effects of photodegradation were relevant (Stubbins et al., 2006; Xu et al., 2020; Wilske et al., 2020), further corroborating the reduced impact of photodegradation on the DOM accumulated in brines.

The accumulation of saturated (low DBE) and relatively oxidized (high NOSC) molecules and the absence of aromatic-like substances (i.e., $AI_{mod} = 0$) in the brines as well as the increase in the relative contribution of highly oxygenated MFs are evidencing in-depth transformation of the DOM pool during drying and simultaneous exacerbation of salinity (Jiang et al., 2022). As mentioned previously, halophytic communities in highly dynamic saline-hypersaline lagoons typically counteract external osmotic stress by accumulating a high amount of small-sized organic solutes (Roberts, 2005). All these osmolytes (polyols, sugars, betaines and ectoines) and their hydrolyzed derivatives are non-aromatic compounds (i.e., $AI_{mod} = 0$) and most are

Table 2
Molecular characterization of SPE-DOM obtained from La Salineta. The molecular class criteria and SPE-DOM descriptors are defined in Table SI4. All values are signal intensity weighted. CA: condensed and aromatic-like moieties. HO: highly oxygenated molecules.

Samples	Richness	Mass	H/C	O/C	C/N	DBE	AI_{mod}	NOSC	CHO%	CHNO%	CHNOS%	CHOS%	CRAM%	Aromatics%	CA%	Aliphatics%	HO%
Salt crust leachate	5453	354.6	1.36	0.5	29.2	6.45	0.17	−0.22	57.4	25.6	2	15	46.3	2.63	0.37	19.5	0.21
Sup28/01	5723	370.4	1.32	0.5	42.6	7.01	0.2	−0.23	62.3	21.8	2.3	13.6	54.8	2.65	0.43	14.2	0.18
Sup21/05	5505	366.7	1.34	0.51	46.6	6.75	0.18	−0.23	62.5	19.8	2.6	15.2	51.2	1.78	0.21	16.3	0.26
Sup15/06	5913	368.8	1.32	0.54	41.3	6.87	0.18	−0.14	60.5	21.5	2.9	15.1	48.9	1.94	0.29	13.6	0.37
Sup30/06	5622	360	1.31	0.55	34.5	6.79	0.18	−0.09	57.7	23.7	3.5	15.1	48.6	2.2	0.35	12.3	0.69
Sup09/10	5768	357	1.31	0.55	33.3	6.73	0.18	−0.08	56.2	23.8	4.1	16	48.4	2.3	0.34	12.1	0.86
Sup29/12	4631	353.7	1.38	0.48	50.0	6.27	0.17	−0.32	61.5	18.1	2.4	18.1	49.6	1.5	0.12	22.34	0.19
Int30/06	5377	360.9	1.29	0.53	37.7	6.98	0.2	−0.12	60	22.7	3.2	14.1	52.9	2.75	0.44	10.5	0.38
Int20/07	4068	357.6	1.29	0.54	44.0	6.91	0.2	−0.12	62.8	21.1	2.4	13.7	52.8	2.34	0.26	10	0.21
Int09/10	4946	353.8	1.28	0.57	34.1	6.83	0.19	−0.02	57.6	24	3.7	14.7	48.4	2.64	0.39	9.1	0.81
Int29/12	5850	368.7	1.24	0.55	35.7	7.45	0.22	−0.03	59.4	23.3	3.5	13.8	56.7	3.36	0.53	5.8	0.75

See SI5 for molecular classes constrains.

oxidized (i.e., O/C > 0.5 and NOSC > 0).

The Spearman rank analysis selected 26 highly oxygenated MFs that significantly and positively correlated with the DOC concentration. Moreover, relative peak intensity of S-bearing highly oxygenated molecules was higher than that of CHO analogous. Are these molecules mirroring the release of osmolytes from decaying planktonic microbiota due to the increase in salinity? Simultaneously, does the abundance of CHOS highly oxygenated molecules indicating that these compounds are susceptible to be sulfurized by microbiota or by sulfide rich anoxic waters (Gomez-Saez et al., 2017)? Almost nothing is known about how and if osmolytes in these systems are released, degraded and transformed. It is important to remark that most of the osmolytes are typically smaller than 200 Daltons. Therefore, they are out of the detectable mass range for the FT-ICR-MS method used in this study. However, in all samples we identified the MF $C_{12}H_{18}O_6$. To our best knowledge this MF has not been reported in freshwater ecosystems such as reservoirs (Dadi et al., 2017) and might be a putative a three units of the glycerol-based molecule PHB $(C_4H_6O_2)_3$, a well-known carbon reservoir for salt-adapted microorganisms that acts as an osmolyte at high salinity (Roberts, 2005). Moreover, in all samples we also identified the MFs $C_{12}H_{20}O_7$ and $C_{12}H_{18}O_9S$ that might the putative hydrolyzed ($+H_2O$) and sulfurized- ($+SO_3$) molecules, respectively of $(C_4H_6O_2)_3$. Among salt-adapted microbiota, halobacteria and halomonas are known to accumulate PHB (Quillaguamán et al., 2010; Fernandez-Castillo et al., 1986; Abd El-malex et al., 2020) and both have been reported at relatively high abundances in Monegros H-SEAS lakes (including La Salineta; Menéndez-Serra et al., 2020). We did not investigate the molecular structure of this molecule and, caution is needed when relating a molecular formula identified by FT-ICR-MS to a specific compound. However, the ubiquity of peaks identified as corresponding to putative PHB represents an intriguing starting point for future investigations aiming to evaluate the hypothesis that the release of osmolytes from halophytic live and decaying microbiota might be key to understanding the production, accumulation and fate of DOC in hypersaline waters.

As indicated by the isotopic signal of dD and $d^{18}O$, Storm Gloria caused the input of completely "new water". The DOM detected under this wet condition showed the highest aromaticity, humification and unsaturation degree, with the relative contribution of CRAM-like substances being the highest and that of the highly oxygenated ones being the lowest. Storm Gloria could have led to surface runoff from the surrounding flat lands of the playa lake, with the subsequent input of terrigenous aromatic and unsaturated organic substances. By contrast, the DOM obtained after the rewetting caused by the autumn rains did not show this consistent terrigenous signature. The signal of dD and $d^{18}O$ in this sample revealed the input of "new" water, but the isotopic signature was slightly separated from the meteoric water line, indicating a mixture of "new" rain with "old" water from the residual brines. As a consequence, the autumnal rewetting was not a severe flushing episode that dragged terrestrial material/solutes from the surrounding lands. Interestingly, FT-ICR-MS revealed that the SPE-DOM of the autumnal rewetting water shared molecular characteristics observed in the SPE-DOM obtained from the salt crust leachate, indicating that the redissolution of the SPE-DOM trapped in the salt crust during the previous dry period might partly explain the properties of the DOM obtained from the autumnal rewetting conditions. Therefore, this "old" DOM might help to sustain the new planktonic heterotrophs proliferating in the water column during rewetting.

The DOM from the salt crust sample stood out for having a large proportion of N (i.e., the lowest C/N ratio in the SPE-DOM and in the bulk DOM) with respect to that of the brines. In addition, fluorescence analysis revealed a significantly stronger signal for protein-like fluorophores. Since this information came from only one sample, it is only preliminary and indicates that the high salinity found at La Salineta may cause the sequestration of N-bearing molecules in the salt crust, resulting in a qualitative shift of the DOM pool. This result is consistent with the salting-out phenomenon, which is well recognized by chemists and is

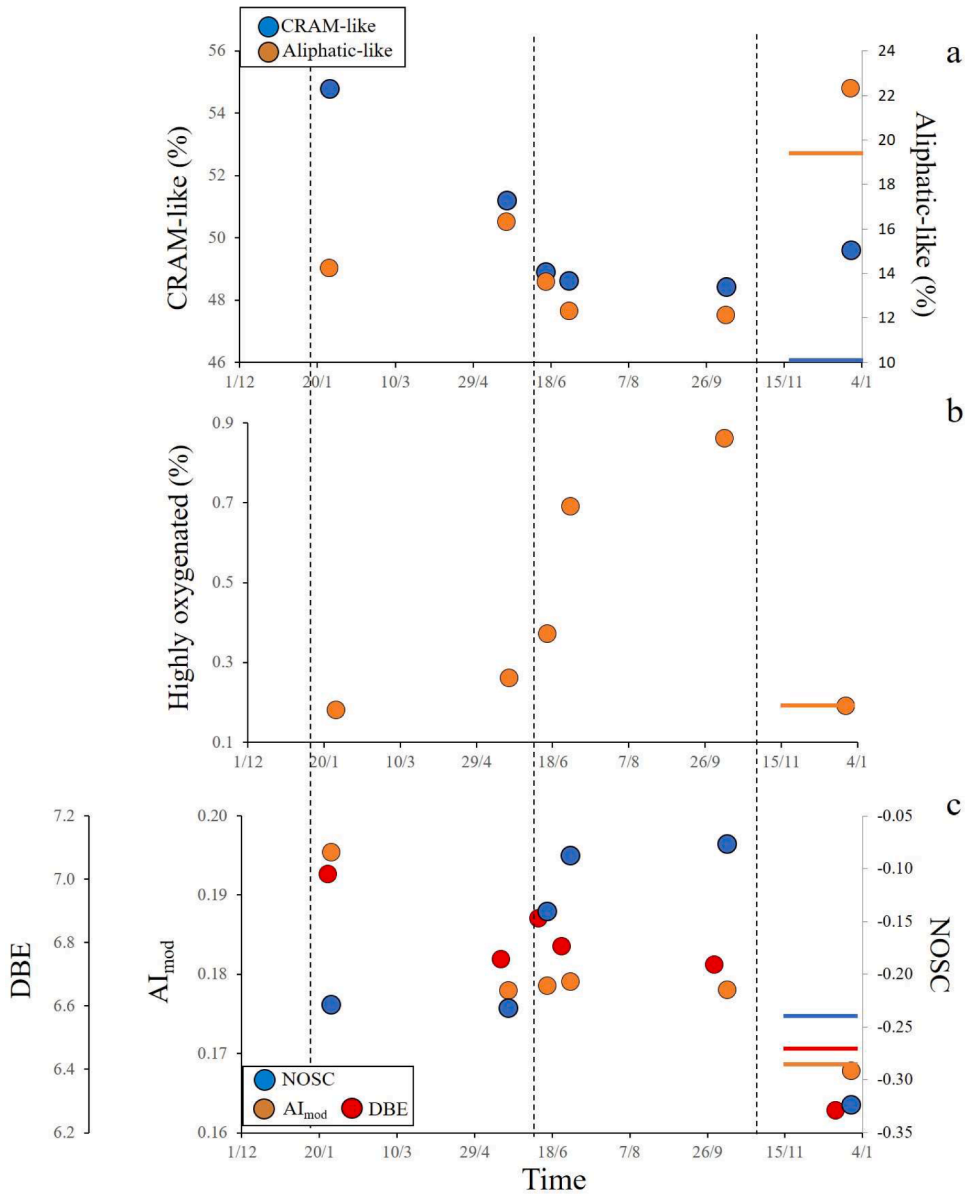

Fig. 7. Temporal dynamics of several SPE-DOM molecular classes and descriptors in surface waters during the study period. Horizontal colored segments on the right of each plot indicate the value of these parameters in the SPE-DOM from the salt crust leachate.
The three vertical dashed lines (from left to right) indicate the timing of Storm Gloria, the formation of brines and autumnal rewetting, respectively.

used in the purification of chemicals (Grover and Ryall, 2005) and the reduction of organic contaminants in aquatic ecosystems (Xie et al., 1997). However, to our knowledge, our report is the first to provide preliminary findings that this phenomenon could be relevant in controlling the quality of DOM in H-SEAS. In the near future, it will be significant to explore how salinity affects the structure of DOM molecules and if these putative alterations modify its bioavailability to halophytic heterotrophic bacteria.

Going beyond and placing our results in a more global context, SPE-DOM from La Salineta showed very low aromaticity (low AI_{mod}), even lower than that previously reported for a highly productive saline soda lake (Butturini et al., 2020), and a relatively high oxidation state (NOSC) that was similar to that reported for streams/small rivers that are usually not affected much by photodegradation (Fig. 9). Therefore, the accumulation of oxidized and non-aromatic moieties in La Salineta, especially in brines, emerges as an outstanding distinctive biogeochemical signature of H-SEAS, providing further evidence of the uniqueness of these extreme and fragile ecosystems. Caution must be taken when comparing results obtained with different instrumentations, different extraction protocols, different data analysis tools or different habitats (see Jian et al., 2022 for more details about some technical drawbacks). In our example, to constrain these limitations we used data obtained from only two studies: one that describe data from a variety of freshwater systems across United States (Kellerman et al., 2018) and the second one from a productive saline soda lake (Butturini et al., 2020) which applied the same instrumentation and identical solid-phase extraction protocol of the present study. Be aware on the need to solve the technical limitations, to advance in our understanding of how DOM molecular chemodiversity change across aquatic ecosystems, it will be essential to promote more accurate and exhaustive comparative studies integrating the larger variety of ecosystems and, therefore expanding our studies to more anomalous habitats such as the hypersaline water bodies.

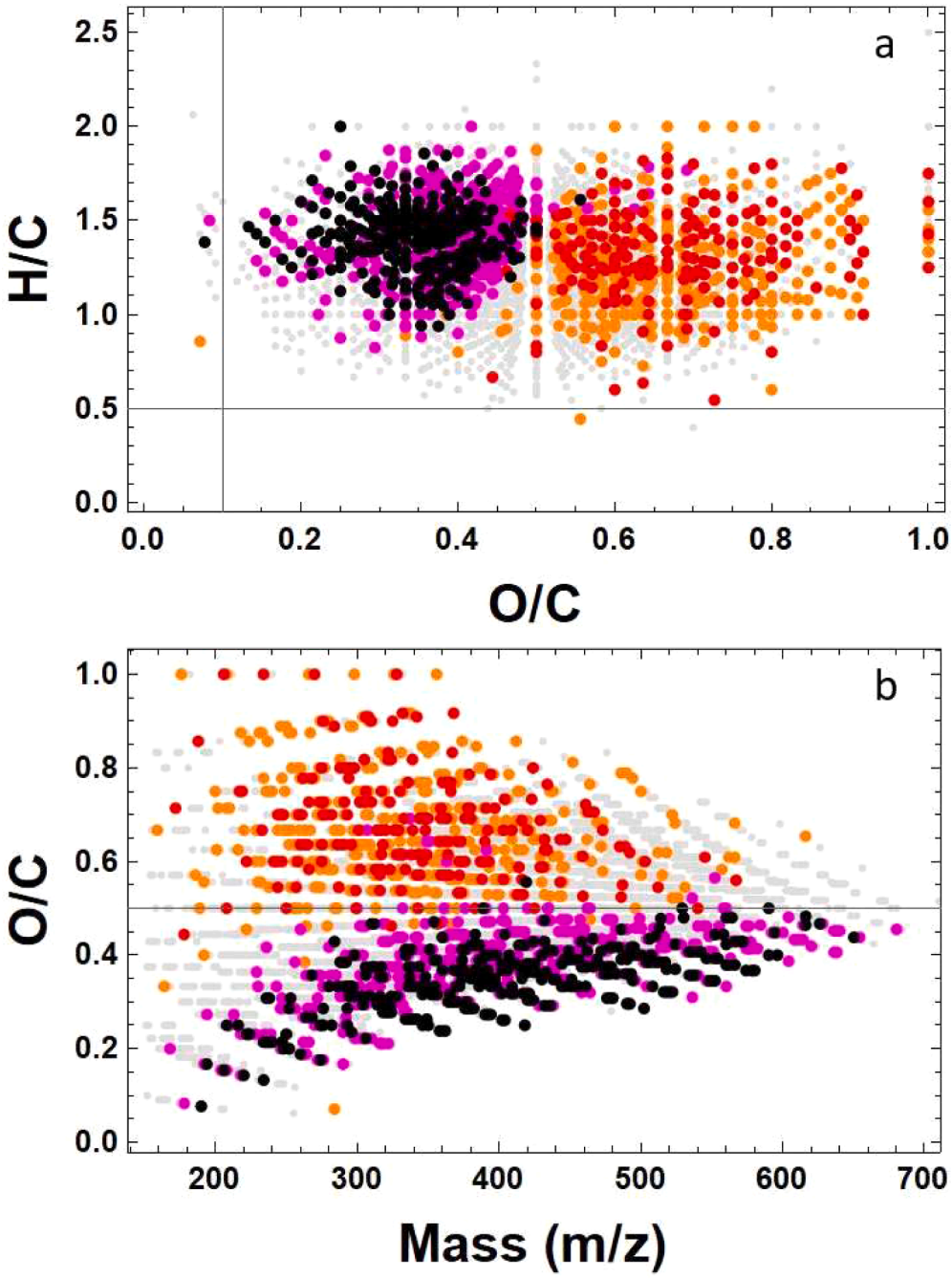

Fig. 8. Van Krevelen (panel a) and the O/C ratio vs the mass (panel b) of all the MFs identified with FT-ICR-MS in the surface waters. Colors indicate the significance level of the Spearman correlations between the relative abundance of the molecules and the DOC concentration. Red and orange: positive correlations, $p < 0.005$ and $0.005 < p < 0.01$, respectively. Black and magenta: negative correlations, $p < 0.005$ and $0.005 < p < 0.01$, respectively. Gray dots: no correlations ($p > 0.01$).

5. Conclusions

(1) The evaporative cycle in a shallow hypersaline lake culminated with the formation of a dense salt-saturated and organic-rich solution. High evaporation converted the playa lake into a natural "reactor", with a disproportionate excess of DOC under the most extreme hypersaline conditions.

(2) A temporal asynchrony was observed between the temporal dynamics in the DOC concentration and DOM qualitative proxies, with most of the qualitative changes in the DOM preceded by the quantitative ones. This asynchrony likely reflects the prevalence of DOM photodegradation at the beginning of the hydrological cycle and the delayed DOM accumulation of fresh autochthonous substances coinciding with the net DOC accrual during dry conditions.

(3) Oxidized, small, no-aromatic and saturated SPE-DOM molecules tended to covary positively with the DOC concentration and accumulated in brines. The relative contribution of highly oxygenated (O/C>0.9) molecules increased remarkably under high DOC concentrations.

(4) The presence of highly oxygenated molecules together with the occurrence of putative PBH (and its hydrolyzed and sulfonated derivates) suggested that the DOM released by live and decaying microplankton is key to understanding the excess of DOC and the properties of DOM in hypersaline endorheic playa lakes.

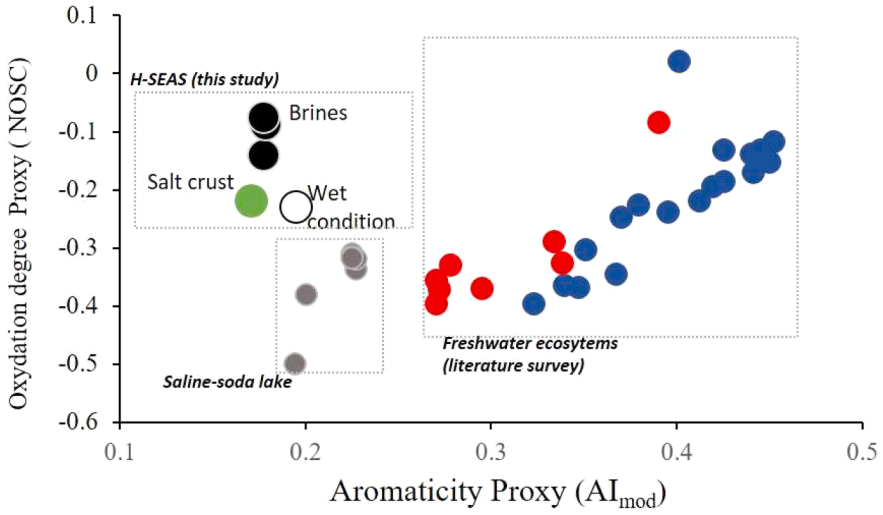

Fig. 9. Relationship between the aromatic degree (AI_{mod}) and the carbon oxidation state (NOSC) in streams/rivers (blue dots), lakes and reservoirs (red dots), a tropical saline soda lake (gray dots) and La Salineta (larger white, black and green dots). Data from the rivers, lakes, reservoirs and the saline soda lake are from Kellerman et al. (2018) and Butturini et al. (2020).

Declaration of Competing Interest

The authors declare that they have no known competing financial interests or personal relationships that could have appeared to influence the work reported in this paper.

Acknowledgments

The grant RTI2018-097950-B-C21/C22 (DryHarshSal Project) from MCIN/AEI/10.13039/501100011033 funded this study. We gratefully acknowledge Jan Kaesler for his help with the FT-ICR-MS and the center for Chemical Microscopy (ProVIS) at the Helmholtz center for Environmental Research, Leipzig (Germany), supported by European Regional Development Funds (EFRE - Europe Funds Saxony) and the Helmholtz Association. We thank the Instituto Aragonés de Gestión Ambiental (INAGA) for facilitating access to the study site, AEMET for the meteorological data, and Ariadna Vidal for performing the spectroscopic analyses. Finally, we thank three anonymous reviewers for constructive comments to further improve the manuscript.

Supplementary materials

Supplementary material associated with this article can be found, in the online version, at doi:10.1016/j.watres.2022.118727.

References

Abd El-malek, F., Farag, A., Omar, S., Khairy, H., 2020. Polyhydroxyalkanoates (PHA) from Halomonas pacifica ASL10 and Halomonas salifodiane ASL11 isolated from Mariout salt lakes. Int. J. Biol. Macromol. 161, 1318–1328.

Altendorf, K., Booth, I.R., Gralla, J.A.Y., Greie, J.C., Rosenthal, A.Z., Wood, J.M., 2009. Osmotic stress. Ecosal Plus 3 (2).

Araguas-Araguas, L.J., Diaz Teijeiro, M.F., 2005. Isotope composition of precipitation and water vapour in the Iberian Peninsula: first results of the Spanish network of isotopes in precipitation. Int. At. Energy Agency Tech. Rep. 1453, 173–190.

Belilla, J., Iniesto, M., Moreira, D., Benzerara, K., López-García, J.M., López-Archilla, A. I., López-García, P., 2021. Archaeal overdominance close to life-limiting conditions in geothermally influenced hypersaline lakes at the Danakil depression. Ethiopia. Environ. Microbiol. 23 (11), 7168–7182.

Bardavid, R.E., Khristo, P., Oren, A., 2008. Interrelationships between Dunaliella and halophilic prokaryotes in saltern crystallizer ponds. Extremophiles 12 (1), 5–14.

Boros, E., V.-Balogh, K., Csitári, B., Vörös, L., Székely, A.J., 2020. Macrophytes and groundwater drive extremely high organic carbon concentration of soda pans. Freshw. Biol. 65 (9), 1555–1568.

Butturini, A., Alvarez, M., Bernal, S., Vazquez, E., Sabater, F., 2008. Diversity and temporal sequences of forms of DOC and NO_3-discharge responses in an intermittent stream: predictable or random succession? J. Geophys. Res. Biogeosci. 113 (G3).

Butturini, A., Herzsprung, P., Lechtenfeld, O.J., Venturi, S., Amalfitano, S., Vazquez, E., Fazi, S., 2020. Dissolved organic matter in a tropical saline-alkaline lake of the East African Rift Valley. Water Res. 173, 115532.

Castañeda, C., Herrero, J., 2005. The water regime of the Monegros playa-lakes as established from ground and satellite data. J. Hydrol. 310 (1–4), 95–110.

Chen, W., Westerhoff, P., Leenheer, J.A., Booksh, K., 2003. Fluorescence excitation–emission matrix regional integration to quantify spectra for dissolved organic matter. Environ. Sci. Technol. 37 (24), 5701–5710.

Conesa Mor, J.A., Castañeda del Álamo, C., Pedrol Solanes, J., 2011. Las Saladas De Monegros y su entorno: Hábitats y Paisaje Vegetal. Consejo de Protección de la Naturaleza de Aragón, p. 538.

Craft, K.M., Horel, J.D., 2019. Variations in surface albedo arising from flooding and desiccation cycles on the Bonneville Salt Flats, Utah. J. Appl. Meteorol. Climatol. 58 (4), 773–785.

Dadi, T., Harir, M., Hertkorn, N., Koschorreck, M., Schmitt-Kopplin, P., Herzsprung, P., 2017. Redox conditions affect DOC quality in stratified freshwaters. Environ. Sci. Technol. 51, 13705–13713.

Da Silva, M.P., Blaurock, K., Beudert, B., Fleckenstein, J.H., Hopp, L., Peiffer, S., Reemtsma, T., Lechtenfeld, O.J., 2021. Delineating source contributions to stream dissolved organic matter composition under baseflow conditions in forested headwater catchments. J. Geophys. Res. Biogeosci. https://doi.org/10.1029/2021JG006425.

Da Silva, M.P., Kaesler, J.M., Reemtsma, T., Lechtenfeld, O.J., 2020. Absorption mode spectral processing improves data quality of natural organic matter analysis by Fourier-transform ion cyclotron resonance mass spectrometry. Journal of the American Society for Mass Spectrometry 31 (7), 1615–1618.

Del Vecchio, R., Blough, N.V., 2006. Influence of ultraviolet radiation on the chromophoric dissolved organic matter in natural waters. Environmental UV Radiation: Impact on Ecosystems and Human Health and Predictive Models. Springer, Dordrecht, pp. 203–216.

Dittmar, T., Koch, B., Hertkorn, N., Kattner, G., 2008. A simple and efficient method for the solid-phase extraction of dissolved organic matter (SPE-DOM) from seawater. Limnol. Oceanogr. Methods 6 (6), 230–235.

Domínguez-Beisiegel, M., Castañeda, C., Herrero, J., 2013. Two microenvironments at the soil surface of saline wetlands in Monegros, Spain. Soil Sci. Soc. Am. J. 77 (2), 653–663.

Fazi, S., Amalfitano, S., Venturi, S., Pacini, N., Vazquez, E., Olaka, L.A., Butturini, A., 2021. High concentrations of dissolved biogenic methane associated with cyanobacterial blooms in East African lake surface water. Comm. Biol. 4 (1), 1–12.

Fernandez-Castillo, R., Rodriguez-Valera, F., Gonzalez-Ramos, J., Ruiz-Berraquero, F., 1986. Accumulation of poly (β-hydroxybutyrate) by halobacteria. Appl. Environ. Microbiol. 51 (1), 214–216.

Gardecki, J.A., Maroncelli, M., 1998. Set of secondary emission standards for calibration of the spectral responsivity in emission spectroscopy. Appl. Spectrosc. 52 (9), 1179–1189.

Goletz, C., Wagner, M., Grübel, A., Schmidt, W., Korf, N., Werner, P., 2011. Standardization of fluorescence excitation–emission-matrices in aquatic milieu. Talanta 85 (1), 650–656.

Gomez-Saez, G.V., Pohlabeln, A.M., Stubbins, A., Marsay, C.M., Dittmar, T., 2017. Photochemical alteration of dissolved organic sulfur from sulfidic porewater. Environ. Sci. Technol. 51 (24), 14144–14154.

Gonsior, M., Schmitt-Kopplin, P., Bastviken, D., 2013. Depth-dependent molecular composition and photo-reactivity of dissolved organic matter in a boreal lake under winter and summer conditions. Biogeosciences 10 (11), 6945–6956.

Grover, P.K., Ryall, R.L., 2005. Critical appraisal of salting-out and its implications for chemical and biological sciences. Chem. Rev. 105 (1), 1–10.

Helms, J.R., Stubbins, A., Ritchie, J.D., Minor, E.C., Kieber, D.J., &Mopper, K., 2008. Absorption spectral slopes and slope ratios as indicators of molecular weight, source, and photobleaching of chromophoric dissolved organic matter. Limnol. Oceanogr. 53 (3), 955–969.
Herzsprung, P., von Tümpling, W., Hertkorn, N., Harir, M., Büttner, O., Bravidor, J., Friese, K., Schmitt-Kopplin, P., 2012. Variations of DOM quality in inflows of a drinking water reservoir: linking of van Krevelen diagrams with EEMF spectra by rank correlation. Environ. Sci. Technol. 46 (10), 5511–5518.
Herzsprung, P., Hertkorn, N., von Tümpling, W., Harir, M., Friese, K., Schmitt-Kopplin, P., 2014. Understanding molecular formula assignment of Fourier transform ion cyclotron resonance mass spectrometry data of natural organic matter from a chemical point of view. Anal. Bioanal. Chem. 406 (30), 7977–7987.
Herzsprung, P., Osterloh, K., von Tümpling, W., Harir, M., Hertkorn, N., Schmitt-Kopplin, P., Meissner, R., Bernsdorf, S., Friese, K., 2017. Differences in DOM of rewetted and natural peatlands – results from high-field FT-ICR-MS and bulk optical parameters Sci. Total Environ., 586, 770–781.
Herzsprung, P., Wentzky, V.C., Kamjunke, N., von Tümpling, W., Wilske, C., Friese, K., Boehrer, B., Reemtsma, T., Rinke, K., Lechtenfeld, O.J., 2020. Improved understanding of dissolved organic matter processing in freshwater using complementary experimental and machine learning approaches. Environ. Sci. Technol. 54 (21), 13556–13565.
Huguet, A., Vacher, L., Relexans, S., Saubusse, S., Froidefond, J.M., Parlanti, E., 2009. Properties of fluorescent dissolved organic matter in the Gironde Estuary. Org. Geochem. 40 (6), 706–719.
Jiang, H., Lv, Q., Yang, J., Wang, B., Dong, H., Gonsior, M., Schmitt-Kopplin, P., 2022. Molecular composition of dissolved organic matter in saline lakes of the Qing-Tibetan plateau. Org. Geochem. 167, 104400.
Kellerman, A.M., Guillemette, F., Podgorski, D.C., Aiken, G.R., Butler, K.D., Spencer, R. G., 2018. Unifying concepts linking dissolved organic matter composition to persistence in aquatic ecosystems. Environ. Sci. Technol. 52, 2538–2548.
Koch, B.P., Dittmar, T., 2016. Erratum: from mass to structure: an aromaticity index for high-resolution mass data of natural organic matter. Rapid Commun. Mass Spectrom. 30, 250. https://doi.org/10.1002/rcm.7433.
Lakowicz, J.R., 2006. Principles of Fluorescence Spectroscopy, 3rd ed. Springer. URL. http://www.springer.com/chemistry/analytical+chemistry/book/978-0-387-31278-1.
LaRowe, D.E., Van Cappellen, P., 2011. Degradation of natural organic matter: a thermodynamic analysis. Geochim. Cosmochim. Acta 75, 2030–2042.
Larsson, T., Wedborg, M., Turner, D., 2007. Correction of inner-filter effect in fluorescence excitation-emission matrix spectrometry using Raman scatter. Anal. Chim. Acta 583 (2), 357–363.
Lawaetz, A.J., Stedmon, C.A., 2009. Fluorescence intensity calibration using the Raman scatter peak of water. Appl. Spectrosc. 63 (8), 936–940.
Lechtenfeld, O.J., Koch, B.P., Gašparović, B., Frka, S., Witt, M., Kattner, G., 2013. The influence of salinity on the molecular and optical properties of surface microlayers in a karstic estuary. Mar. Chem. 150, 25–38.
Lechtenfeld, O.J., Hertkorn, N., Shen, Y., Witt, M., Benner, R., 2015. Marine sequestration of carbon in bacterial metabolites. Nat. Commun. 6, 6711.
Lee, C.J., McMullan, P.E., O'Kane, C.J., Stevenson, A., Santos, I.C., Roy, C., Hallsworth, J. E., 2018. NaCl-saturated brines are thermodynamically moderate, rather than extreme, microbial habitats. FEMS Microbiol. Rev. 42 (5), 672–693.
Li, W., Zhou, R., Mu, Y., 2012. Salting effects on protein components in aqueous NaCl and urea solutions: toward understanding of urea-induced protein denaturation. J. Phys. Chem. B 116 (4), 1446–1451.
Lopez, P.L., Mandado, J.M., 2007. Experimental evaporation of superficial brines from continental playa–lake systems located in Central Ebro Basin (northeast Spain). Geol. Soc. Spec. Publ. 285 (1), 143–154.
Mariot, M., Dudal, Y., Furian, S., Sakamoto, A., Vallès, V., Fort, M., Barbiero, L., 2007. Dissolved organic matter fluorescence as a water-flow tracer in the tropical wetland of Pantanal of Nhecolândia, Brazil. Sci. Total Environ. 388 (1–3), 184–193.
McKnight, D.M., Boyer, E.W., Westerhoff, P.K., Doran, P.T., Kulbe, T., Andersen, D.T., 2001. Spectrofluorometric characterization of dissolved organic matter for indication of precursor organic material and aromaticity. Limnol. Oceanogr. 46 (1), 38–48.
Menéndez-Serra, M., Triadó-Margarit, X., Casamayor, E.O., 2021. Ecological and metabolic thresholds in the bacterial, protist, and fungal microbiome of ephemeral saline lakes (Monegros Desert, Spain). Microb. Ecol. 1–12.
Menéndez-Serra, M., Ontiveros, V.J., Triadó-Margarit, X., Alonso, D., Casamayor, E.O., 2020. Dynamics and ecological distributions of the Archaea microbiome from inland saline lakes (Monegros Desert, Spain). FEMS Microb. Ecol. 96 (3) fiaa019.
Messager, M.L., Lehner, B., Grill, G., Nedeva, I., Schmitt, O., 2016. Estimating the volume and age of water stored in global lakes using a geo-statistical approach. Nat. Commun. 7 (1), 1–11.
Morling, K., Herzsprung, P., Kamjunke, N., 2017a. Discharge determines production of, decomposition of and quality changes in dissolved organic carbon in pre-dams of drinking water reservoirs. Sci. Total Environ. 577, 329–339.
Morling, K., Raeke, J., Kamjunke, N., Reemtsma, T., Tittel, J., 2017b. Tracing aquatic priming effect during microbial decomposition of terrestrial dissolved organic carbon in chemostat experiments. Microb. Ecol. 74, 534–549.
Murtagh, F., Legendre, P., 2014. Ward's hierarchical agglomerative clustering method: which algorithms implement Ward's criterion? J. Class. 31 (3), 274–295.
Ohno, T., 2002. Fluorescence inner-filtering correction for determining the humification index of dissolved organic matter. Environ. sci. & Tech. 36 (4), 742–746.
Osburn, C.L., Wigdahl, C.R., Fritz, S.C., Saros, J.E., 2011. Dissolved organic matter composition and photoreactivity in prairie lakes of the US Great Plains. Limnol. Oceanogr. 56 (6), 2371–2390.
Orellana, M.V., Pang, W.L., Durand, P.M., Whitehead, K., Baliga, N.S., 2013. A role for programmed cell death in the microbial loop. PLoS ONE 8 (5), e62595.
Oren, A., 1993. Availability, uptake and turnover of glycerol in hypersaline environments. FEMS Microb. Ecol. 12, 15–23.
Quillaguamán, J., Guzmán, H., Van-Thuoc, D., Hatti-Kaul, R., 2010. Synthesis and production of polyhydroxyalkanoates by halophiles: current potential and future prospects. Applied microbiology and biotechnology 85 (6), 1687–1696.
Reardon, J. (1969). U.S. Patent No. 3,432,395. Washington, DC: U.S. Patent and Trademark Office.
Roberts, M.F., 2005. Organic compatible solutes of halotolerant and halophilic microorganisms. Saline Syst. 1 (1), 1–30.
Rossel, P.E., Stubbins, A., Rebling, T., Koschinsky, A., Hawkes, J.A., Dittmar, T., 2017. Thermally altered marine dissolved organic matter in hydrothermal fluids. Org. Geochem. 110, 73–86.
Rubel, F., Kottek, M., 2010. Observed and projected climate shifts 1901–2100 depicted by world maps of the Köppen-Geiger climate classification. Meteorol. Z. 19 (2), 135.
Salvany, J.M., García-Vera, M.A., Samper, J., 1995. Geología e hidrogeología de la zona endorreica de Bujaraloz-Sástago. Acta Geol. Hislpánica 30, 31–50.
Song, K., Shang, Y., Wen, Z., Jacinthe, P.A., Liu, G., Lyu, L., Fang, C., 2019. Characterization of CDOM in saline and freshwater lakes across China using spectroscopic analysis. Water Res. 150, 403–417.
Stubbins, A., Uher, G., Law, C.S., Mopper, K., Robinson, C., Upstill-Goddard, R.C., 2006. Open-ocean carbon monoxide photoproduction. Deep Sea Research Part II. Trop. Stud. Oceanogr. 53 (14–16), 1695–1705.
Vähätalo, A.V., Wetzel, R.G., 2008. Long-term photochemical and microbial decomposition of wetland-derived dissolved organic matter with alteration of 13C: 12C mass ratio. Limnol. Oceanogr. 53 (4), 1387–1392.
Wang, J., Song, C., Reager, J.T., Yao, F., Famiglietti, J.S., Sheng, Y., Wada, Y., 2018. Recent global decline in endorheic basin water storages. Nat. Geosc. 11 (12), 926–932.
Weishaar, J.L., Aiken, G.R., Bergamaschi, B.A., Fram, M.S., Fujii, R., Mopper, K., 2003. Evaluation of specific ultraviolet absorbance as an indicator of the chemical composition and reactivity of dissolved organic carbon. Environm. Sci. Technol. 37 (20), 4702–4708.
Wen, Z., Song, K., Shang, Y., Zhao, Y., Fang, C., Lyu, L., 2018. Differences in the distribution and optical properties of DOM between fresh and saline lakes in a semi-arid area of Northern China. Aquat. Sci. 80 (2), 1–12.
Wilske, C., Herzsprung, P., Lechtenfeld, O.J., Kamjunke, N., von Tuempling, W., 2020. Photochemically induced changes of dissolved organic matter in a humic-rich and forested stream. Water 12 (2), 331 (Basel).
Xie, W.H., Shiu, W.Y., Mackay, D., 1997. A review of the effect of salts on the solubility of organic compounds in seawater. Mar. Environ. Res. 44 (4), 429–444.
Xu, W., Gao, Q., He, C., Shi, Q., Hou, Z.Q., Zhao, H.Z., 2020. Using ESI FT-ICR MS to characterize dissolved organic matter in salt lakes with different salinity. Environ. Sci. Technol. 54 (20), 12929–12937.